Exo84 and Sec5 are competitive regulatory Sec6/8 effectors to the RalA GTPase

Rongsheng Jin[1], Jagath R Junutula[2], Hugo T Matern[2,4], Karen E Ervin[2], Richard H Scheller[2] and Axel T Brunger[1,3,*]

[1]Howard Hughes Medical Institute, Stanford University, Stanford, CA, USA, [2]Genentech Inc., 1 DNA Way, South San Francisco, CA, USA and [3]Departments of Molecular and Cellular Physiology, Neurology and Neurological Science, Stanford Synchrotron Radiation Laboratory, Stanford University, Stanford, CA, USA

The Sec6/8 complex, also known as the exocyst complex, is an octameric protein complex that has been implicated in tethering of secretory vesicles to specific regions on the plasma membrane. Two subunits of the Sec6/8 complex, Exo84 and Sec5, have recently been shown to be effector targets for active Ral GTPases. However, the mechanism by which Ral proteins regulate the Sec6/8 activities remains unclear. Here, we present the crystal structure of the Ral-binding domain of Exo84 in complex with active RalA. The structure reveals that the Exo84 Ral-binding domain adopts a pleckstrin homology domain fold, and that RalA interacts with Exo84 via an extended interface that includes both switch regions. Key residues of Exo84 and RalA were found that determine the specificity of the complex interactions; these interactions were confirmed by mutagenesis binding studies. Structural and biochemical data show that Exo84 and Sec5 competitively bind to active RalA. Taken together, these results further strengthen the proposed role of RalA-regulated assembly of the Sec6/8 complex.

Introduction

Spatial regulation of exocytosis is crucial for a variety of cellular processes, such as synapse formation, synaptic plasticity, neurosecretion, and development and maintenance of cell polarity. The delivery of secretory vesicles to spatially restricted areas of the plasma membrane is a multistage process requiring polarized transport, restricted tethering,

*Corresponding author. Howard Hughes Medical Institute, Department of Molecular and Cellular Physiology, Stanford University, James H Clark Center, E300C, 318 Campus Drive, Stanford, CA 94305-5432, USA.
Tel.: +1 650 736 1031; Fax: +1 650 736 1961;
E-mail: brunger@stanford.edu
[4]Present address: Exelixis Inc., 170 Harbor Way, South San Francisco, CA 94080, USA

docking, and fusion of vesicles to specific regions on the plasma membrane. Each of these steps requires a discrete set of proteins to achieve high specificity. SNARE (soluble NSF attachment protein receptor) proteins mediate late-stage vesicle docking and subsequent fusion (Jahn and Südhof, 1999). The tethering step, which is defined as the initial contact of vesicles via a protein bridge with the target membrane, is probably outside the range of SNARE interactions, and might be a crucial stage at which specificity is conferred. Several multimeric protein complexes, termed tethering complexes, have been shown to be essential for most, if not all, membrane fusion events (Whyte and Munro, 2002). Among them is the Sec6/8 complex, also known as the exocyst complex in yeast, which is the tethering complex responsible for exocytosis at the plasma membrane (TerBush et al, 1996; Kee et al, 1997). The Sec6/8 complex plays a role in the delivery of vesicles to the basal–lateral membrane of polarized epithelial cells (Grindstaff et al, 1998) and functions in neurite outgrowth in the nervous system (Vega and Hsu, 2001).

The Sec6/8 complex comprises eight proteins: Sec3, Sec5, Sec6, Sec8, Sec10, Sec15, Exo70 and Exo84. Many small GTPases interact with the Sec6/8 complex, although the regulation of the Sec6/8 complex is different in mammals and in yeast (Matern et al, 2001). In yeast, the exocyst complex interacts with Sec4 (a Rab GTPase), Rho1, Rho3 and Cdc42 (Novick and Guo, 2002). In contrast, the mammalian Sec3 does not have a Rho1/Cdc42-binding site, and its upstream regulator is currently unknown (Matern et al, 2001). Moreover, the mammalian Sec15 is an effector for active Rab11 (Zhang et al, 2004), the Rho family GTPase TC10 interacts with Exo70 (Inoue et al, 2003) and the ADP-ribosylation factor (ARF) 6 binds Sec10 (Prigent et al, 2003). Interestingly, two subunits of the mammalian Sec6/8 complex, Exo84 and Sec5, are *both* effectors of the active Ral GTPases, which are not found in yeast (Moskalenko et al, 2002, 2003; Sugihara et al, 2002).

Ral GTPases, which comprise the highly similar RalA and RalB isoforms (sharing 82% identity), are members of the Ras superfamily. As is characteristic for all members of the Ras superfamily of GTPases, Ral cycles between an active GTP-bound state and an inactive GDP-bound state, and the nucleotide-dependent conformational changes are confined to two regions, known as switch I and switch II (Vetter and Wittinghofer, 2001). Functionally, Ral GTPases are part of extracellular signaling pathways and are involved in the regulation of a diverse array of cellular processes, including oncogenic transformation, endocytosis, exocytosis and actin-cytoskeleton dynamics, via their interactions with various downstream effector proteins (reviewed in Feig, 2003). Ral–Sec6/8 interactions are crucial for targeting basolateral proteins in polarized MDCK cells. In neuroendocrine PC12 cells, Ral–Sec6/8 interactions are involved in the regulation of exocytosis of secretory granules and are essential for GTP-dependent exocytosis (Moskalenko et al, 2002; Wang et al,

2004a). Interestingly, inhibition of endogenous Ral or Exo84 function partially disrupted the assembly of the Sec6/8 complex (Moskalenko *et al*, 2002, 2003), suggesting that Ral and Exo84 are involved in the regulation of the assembly of the Sec6/8 complex. As mentioned above, Ral GTPases are not present in *Saccharomyces cerevisiae*, suggesting that the involvement of Ral proteins in the regulation of the Sec6/8 complex emerged during evolution of multicellular organisms. Therefore, Ral GTPases may represent a special link between signal transduction pathways and regulation of Sec6/8 functions in higher eukaryotes.

The structure of the Ral-binding domain (RBD) of Sec5 in complex with active RalA provided a first glimpse into the specificity of Sec6/8–RalA interactions (Fukai *et al*, 2003). In an effort to understand the dual-effector mechanism of Ral, we present here the 2.0 Å crystal structure of the Exo84-RBD in complex with guanosine-5′-[β,γ-imido] triphosphate (GMPPNP)-bound RalA. On the basis of structure-based mutagenesis and binding studies, we have identified several key residues that determine the specificity for the Exo84–RalA interactions. Furthermore, we obtained structural and biochemical evidence for competitive binding of Exo84 and Sec5 to active RalA. RalA is the first example of a small GTPase that functions by interacting with two competitive effectors that can also be part of the same multimeric protein complex.

Results and discussion

Crystallization and structure determination
The interaction between Exo84 and RalA was originally identified in a yeast two-hybrid screen, and the RBD of Exo84 was mapped to its N-terminal 389 residues (data not shown). In order to facilitate crystallization, the boundaries of Exo84-RBD were probed by limited proteolysis and deletion mutagenesis. The two minimal Exo84-RBDs (residues 167–286 and 167–279) bind to active RalA with a binding affinity of about 42 nM, which is similar to that of a previously reported larger Exo84-RBD construct (residues 122–333) ($K_d \sim 26$ nM) (Moskalenko *et al*, 2003), demonstrating that the two minimal Exo84-RBD fragments used in our studies are sufficient to interact with RalA (Table I). A sequence alignment of the potential RBD fragment for representative members of the Exo84 family is shown in Figure 1. The Q72L point mutation of RalA was introduced in order to stabilize RalA in the active conformation, in analogy to the constitutively active Ras-Q61L mutant (Frech *et al*, 1994). The fragment of RalA-Q72L consisting of residues 9–183 (simply referred to as RalA in the following) was used for crystallization (Fukai *et al*, 2003).

The complexes of GMPPNP-bound RalA with the two different Exo84-RBD fragments crystallized in a similar condition and the crystals were isomorphous to each other (Table II). The structures of the Exo84-RBD[167–286]:RalA complex and the Exo84-RBD[167–279]:RalA complex were determined to 2.5 and 2.0 Å resolution, respectively (Table III). A representative σ_A-weighted $2F_o-F_c$ electron density map is shown in Figure 2B. There are two Exo84-RBD:RalA complexes in the asymmetric unit, which are related to each other by a local non-crystallographic two-fold symmetry operation. A pairwise structural comparison revealed that the structures of the two complexes are nearly identical. Furthermore, the

Table I Dissociation constants for the binding of RalA variants with Exo84-RBD variants, or with wild-type Sec5-RBD

RalA variants[a]	Exo84-RBD (nM)[b]	Sec5-RBD (nM)[c]
RalA-GMPPNP	42±4	10±1
RalA-GDP	1920±100	1400±75
E38A	*63±8*	*446±25*
E38R	*63±12*	*6540±1000*
A48W	1213±112	28±8
S50W	1243±75	67±2
R52A	770±100	23±3
R52W	37±2	1146±91
K47E	**1550±80**	**101±12**
K47I	**51±12**	**11±1**
N81A	**61±20**	**17±4**
N81R	**864±155**	**16±2**

Exo84 variants[b]	RalA wild type (nM)[a]	RalA-K47I (nM)[a]
Exo84-122/333	26±4	45±6
Exo84-167/286	42±4	51±12
A228W	1300±200	N/A
K233W	1100±500	N/A
K272A	95±12	1090±100
S276W	40±4	N/A

[a]All RalA variants are based on the full-length human RalA. The binding experiments were carried out using GMPPNP-bound RalA, unless noted otherwise. Residues that exclusively interact with Exo84-RBD are shown in bold, and residues that exclusively interact the Sec5-RBD are shown in italics.
[b]Exo84-RBD represents the minimal Ral-binding domain of Exo84, including residues 167–286, unless noted otherwise.
[c]Sec5-RBD is the Ral-binding domain of Sec5, including residues 1–99.

structures of Exo84-RBD[167–286] and Exo84-RBD[167–279] are essentially identical. Therefore, one of the two complexes of the higher resolution structure was used for subsequent analysis.

Structure of the Ral-binding domain of Exo84
The Exo84-RBD adopts a pleckstrin homology (PH) domain fold (Figure 2C) consisting of a seven-stranded β-sandwich that contains two nearly orthogonal antiparallel β-sheets (β1–β4 and β5–β7, respectively) and an abutting C-terminal α-helix. The loop connecting β3/β4 (residues 209–215) has relatively weak electron density that is partially stabilized by a crystal contact. Interestingly, dimeric Exo84-RBD and Exo84-RBD:RalA species were observed in solution (Supplementary Figure 1), as well as in the crystal structure of the Exo84-RBD:RalA complex where two Exo84-RBD monomers form a two-fold symmetry related dimer. The first four β-strands (β1–β4) of the Exo84-RBD pack against each other in the dimer forming a large intermolecular β-sandwich (Figure 2D). The dimerization interface buries a surface area of ∼1300 Å^2 and it primarily involves hydrophobic residues, including Leu174, Phe197, Met199, Leu204, Ala206 and Leu221 from each protomer. Further studies are required to reveal the possible physiological relevance of the observed Exo84-RBD dimerization.

A structural similarity search using the DALI server (http://www.ebi.ac.uk/dali/) revealed that the structure of Exo84-RBD is similar to that of other PH domain proteins, despite the absence of significant primary sequence similarity. The closest structural homolog is the PH domain of Dapp1/Phish in complex with inositol 1,3,4,5-tetrakisphosphate (IP4; PDB entry 1FAO) (Ferguson *et al*, 2000); the
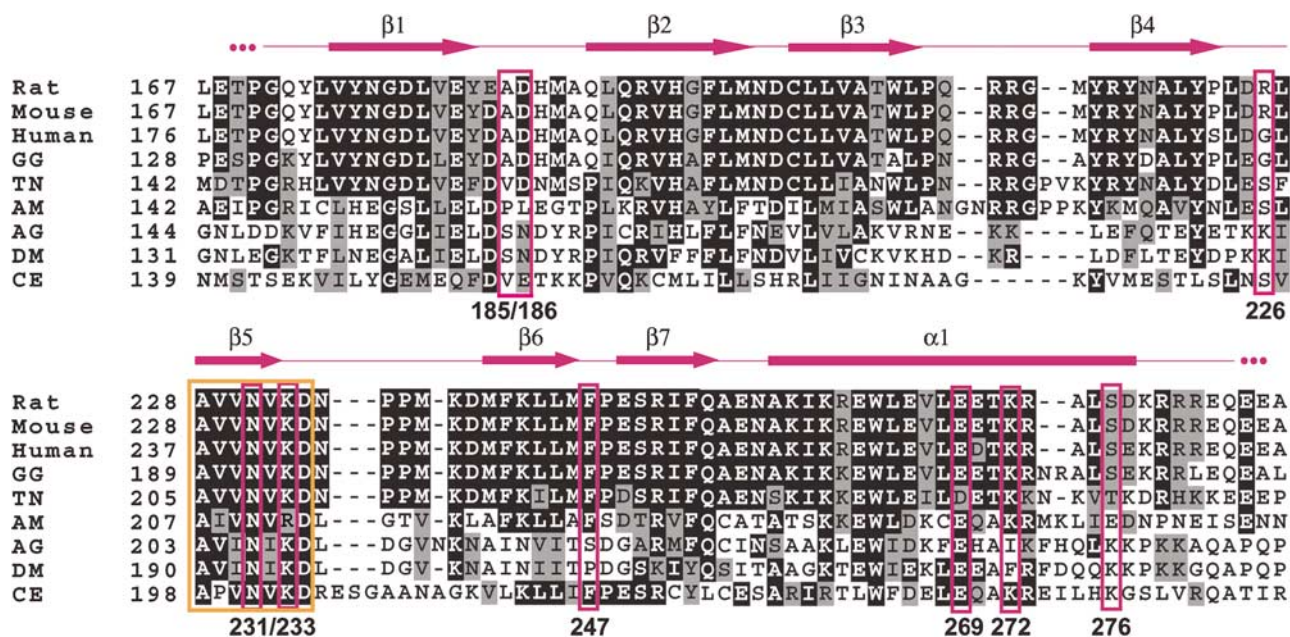
Figure 1 Sequence alignment of the RBDs of representative members of the Exo84 family. The secondary structure of rat Exo84-RBD is shown at the top. Identical residues are shaded in black and similar conserved residues are shaded in gray. The residues of rat Exo84 that directly contact RalA, together with their equivalent residues in other species, are highlighted in red boxes. The highly conserved Exo84 region is indicated with an orange box. The top 10 hits from a two-iteration Blast search (Altschul *et al*, 1997) using full-length rat Exo84 as the bait are *Rattus norvegicus* (rat, NP_620612), *Mus musculus* (mouse, AAH57052), *Homo sapiens* (human, NP_787072), *Gallus gallus* (GG, XP_419572), *Tetraodon nigroviridis* (TN, CAG12974), *Apis mellifera* (AM, XP_395242), *Anopheles gambiae* (AG, XP_313109), *Drosophila melanogaster* (DM, NP_651454), *D. melanogaster* (NP_996299, not shown) and *Caenorhabditis elegans* (CE, NP_493541). The highest sequence identity is between rat and mouse Exo84 (98%), while the lowest is between rat and *C. elegans* proteins (25%). The alignment was made using ClustalW (Thompson *et al*, 1994).

Table II X-ray diffraction data collection statistics

Unit cell dimensions	$a = 52.5$ Å, $b = 113.8$ Å, $c = 71.0$ Å, $\beta = 102.7°$				
Space group	P2$_1$				

	MAD data collection				
	Edge	Peak	Remote	Native-1[a]	Native-2[b]
Wavelength (Å)	0.97927	0.97900	0.89194	0.97945	0.97946
d_{min} (Å)[c]	2.5 (2.59)	2.5 (2.59)	2.5 (2.59)	2.5 (2.57)	2.0 (2.02)
Number of total reflections	178 788	179 187	183 191	140 368	387 689
Number of unique reflections	52 110	52 098	53 208	28 917	57 036
Completeness[d]	91.6 (48.5)	91.6 (49.0)	94.1 (65.1)	99.8 (99.7)	96.1 (70.7)
R_{merge} (%)[d,e]	0.082 (0.334)	0.082 (0.334)	0.085 (0.353)	0.090 (0.444)	0.085 (0.469)

[a]Native-1 is the complex of Exo84-RBD(167–286) and RalA.
[b]Native-2 is the complex of Exo84-RBD(167–279) and RalA.
[c]Values in parentheses define the low-resolution limits for the last shell of the diffraction data.
[d]Values in parentheses are statistics for the last shell of the diffraction data.
[e]$R_{merge} = \sum_h \sum_i |I_{hi} - \langle I_h \rangle| / \sum_h \sum_i |I_{hi}|$.

root-mean-square deviation (r.m.s.d.) calculated for 95 equivalent Cα atoms is 2.9 Å, whereas the sequence identity is only 14%. PH domains are commonly found in eukaryotic signaling proteins. They are best known for their ability to recruit proteins to membranes through their association with membrane phosphatidylinositides, although they can also function as general protein-binding modules (Lemmon and Ferguson, 2000). The structure of the Exo84-RBD:RalA complex shows that a PH domain can also act as an effector to small GTPases, and thus widens the observed functional diversity of PH domains.

PH domains that bind specifically to phosphoinositides comprise only about 10% of the known PH domain proteins

(Lemmon and Ferguson, 2000). The majority only bind phosphoinositides with low affinity and poor specificity. A common feature of many PH domains with known structures is strong surface charge polarization. Three loops (β1/β2, β3/β4 and β6/β7), also termed variable loops since they represent the most variable regions of PH domains, typically form a positively charged surface, and have been implied in binding with membrane phosphoinositides. Despite adopting a typical PH domain fold, such a charge polarization is absent in Exo84-RBD. Furthermore, the variable loops are mostly negatively charged (not shown), suggesting that the conformation of Exo84-RBD as observed here is unlikely to bind individual phospholipid molecules with high affinity or

specificity. Indeed, we were unable to detect any interaction between Exo84-RBD and several inositol phosphates, including IP4, using either isothermal titration calorimetry or surface plasmon resonance (SPR) (data not shown). However, using radiolabeled liposomes, it has been shown that Exo84-

RBD (residues 122–333) interacts with phospholipid membranes *in vitro* (Moskalenko *et al*, 2003). Thus, it appears that in the context of a membrane environment, measurable binding affinity to phospholipids can be induced.

Overview of the Exo84-RBD:RalA complex

The Exo84-RBD:RalA complex is stabilized through extensive intermolecular interactions that bury a solvent-accessible surface area of $\sim 1700\,\text{Å}^2$ (Figure 3A). This is significantly larger than that between Sec5 and RalA ($1000\,\text{Å}^2$), and that between Ras and its effectors ($\sim 1300\,\text{Å}^2$ for PI3Kγ, Raf and RalGDS) (Pacold *et al*, 2000; Fukai *et al*, 2003). Exo84 interacts with both switch regions (Figure 3), unlike Sec5, which primarily interacts with switch I.

A structural comparison with the uncomplexed GDP-bound RalA (Bauer *et al*, 1999; Nicely *et al*, 2004) shows that the largest conformational changes upon GTP binding are exhibited by residues 38–50 and 69–85, which are therefore referred to as RalA switch I and switch II (Figure 2A). Accordingly, we classified the Exo84-RBD:RalA interactions into three categories (Figure 3B). The first group comprises intermolecular interactions involving three RalA residues in switch I, Lys47, Ala48 and Ser50. The second group involves four RalA residues in switch II, Glu73, Tyr75, Asn81, and Tyr82. The third group of interacting residues includes Lys16$^{\text{RalA}}$ and Arg52$^{\text{RalA}}$. Additionally, six well-ordered

Table III Refinement statistics

	Exo84 (167–286):RalA	Exo84 (167–279):RalA
Resolution (Å)	2.5	2.0
R_{work} (%)[a]	20.7	20.6
R_{free} (%)[b]	24.8	23.0
No. of protein atoms	4678	4598
No. of water molecules	153	413
Ligand atoms	2 Mg^{2+} and 2 GMPPNP	2 Mg^{2+} and 2 GMPPNP
Mean B-value (Å^2)	42.9	36.6
R.m.s.d. bond length (Å)	0.0079	0.0079
R.m.s.d. bond angles (deg)	1.25	1.33
Ramachandran statistics		
Most favored (%)	89.0	90.7
Additionally allowed (%)	10.6	8.9
Generally allowed (%)	0.4	0.4

[a]$R_{\text{work}} = (\sum||F_{\text{o}}|-|F_{\text{c}}||)/\sum|F_{\text{o}}|$, where F_{o} and F_{c} denote observed and calculated structure factors, respectively.
[b]A total of 10% of the reflections were set aside for the calculation of R_{free}.

Figure 2 Structure of the Exo84-RBD:RalA complex. (**A**) Ribbon diagram of the Exo84-RBD:RalA complex. Exo84-RBD is colored in red. RalA is colored in green, except that switch I (38–50) and switch II (69–85) are highlighted in orange. The secondary structures of RalA are numbered in a sequential order. The GMPPNP is shown in a ball-and-stick representation and the Mg^{2+} is shown as a gray sphere. A close-up view of the boxed region is shown in panel B, which is superimposed with a portion of electron density map. (**B**) Representative portion of a σ_{A}-weighted $2F_{\text{o}}-F_{\text{c}}$ electron density map (contoured at $1.0\,\sigma$) overlaid with the final refined model. The Exo84 and RalA molecules are colored as in panel A and the selected residues are shown in a ball-and-stick representation. (**C**) Ribbon representation of the Exo84-RBD structure. The secondary structure elements are numbered in a sequential order. (**D**) Exo84-RBD:RalA complex forms a two-fold symmetry related dimer in the crystal. The Exo84-RBD molecules are red and cyan, while the RalA molecules are green and light purple, respectively. Also shown are the two GMPPNP molecules. The putative phospholipid-binding sites are indicated by green oval circles.
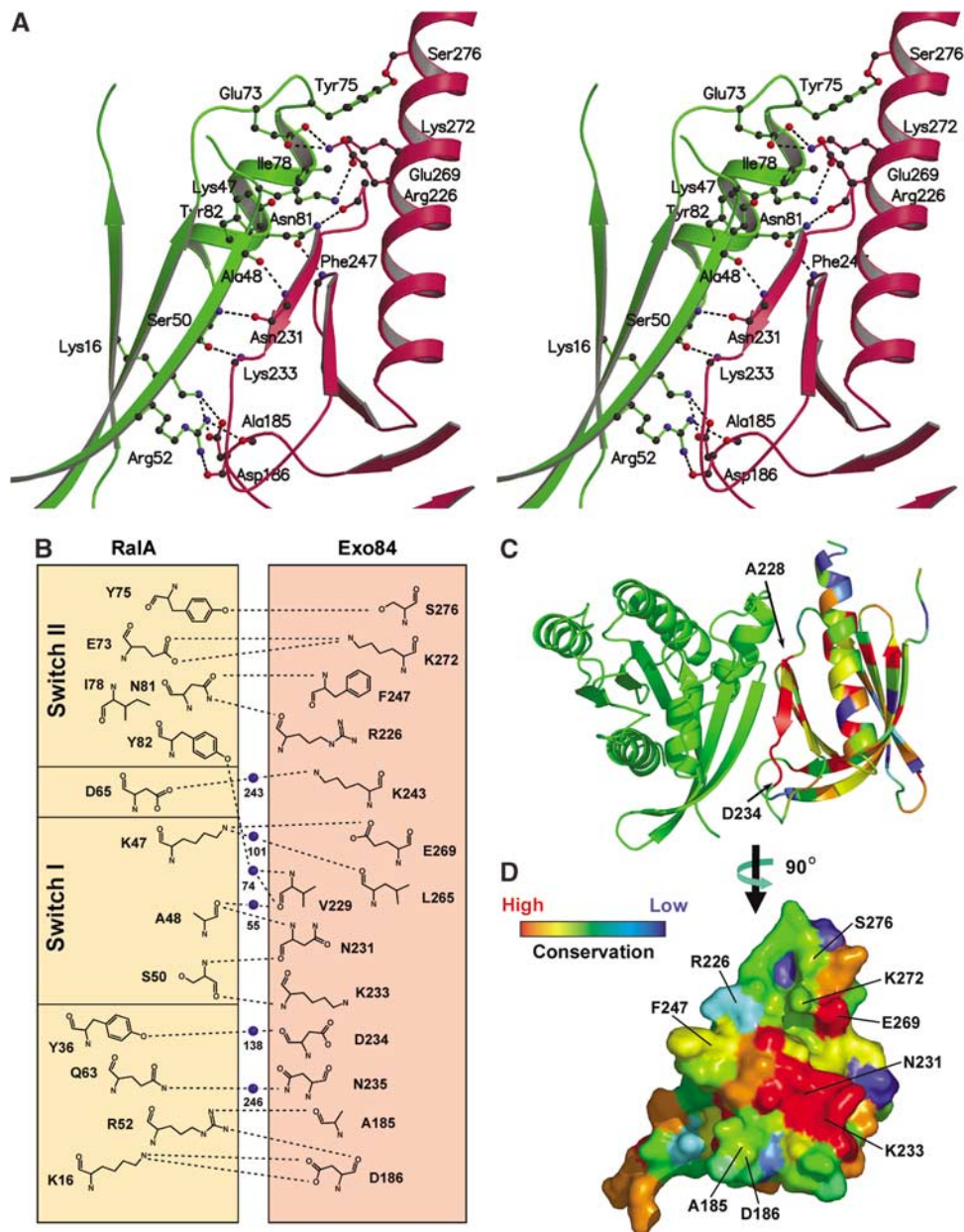
Figure 3 The Exo84-RBD:RalA complex is stabilized by extensive intermolecular interactions. (**A**) Stereo diagram of the interface between Exo84-RBD (red) and RalA (green). Key residues involved in complex interactions are shown in a ball-and-stick representation. Hydrogen bonds and salt bridges are indicated by black dashed lines. The orientation of the complex is similar to that shown in panel C. (**B**) Schematic representation of the Exo84-RBD:RalA interface. Hydrogen bonds and salt bridges are shown as dotted lines between the interacting groups. The water molecules are shown as blue spheres. (**C**) Ribbon representation of the Exo84-RBD:RalA complex. RalA is green. The Exo84-RBD residues are colored according to their conservation while the conservation scores were calculated by ConSurf (Glaser *et al*, 2003). The highest conservation is indicated in red and the lowest is blue. The highly conserved Exo84 motif is indicated. (**D**) Molecular surface of Exo84-RBD with residues colored as in panel C. The Exo84-RBD molecule was rotated about 90° counterclockwise from that shown in panel C. Residues of Exo84-RBD that directly contact RalA are labeled.

water molecules are found near the border of the complex interface (Figure 3B).

The binding sites for Exo84 and Sec5 on RalA are partially overlapping with three RalA residues (Ala48, Ser50 and Arg52) shared by both effectors binding interfaces (Figure 4). These residues discriminate differently between Sec5 and Exo84, which was revealed by mutagenesis studies and measuring the resulting binding affinities by SPR (Table I and Figure 5). For example, A48W^{RalA} and S50W^{RalA} entirely abolish Exo84–RalA binding, but only weakly affect the

Sec5–RalA interaction. This suggests that residues that have relatively small side chains are preferred at these positions for Exo84 binding, while the Sec5–RalA complex is more tolerant to side-chain variations. The opposite result is observed for mutations of Arg52^{RalA}. A tryptophan substitution at Arg52^{RalA} is apparently too bulky to fit in the Sec5–RalA interface, and therefore prevents complex formation. In contrast, RalA-R52W binds to Exo84 with a wild-type-like K_d. R52W^{RalA} is likely involved in hydrophobic interactions with six neighboring Exo84 residues (Met188, Val232, Pro237,
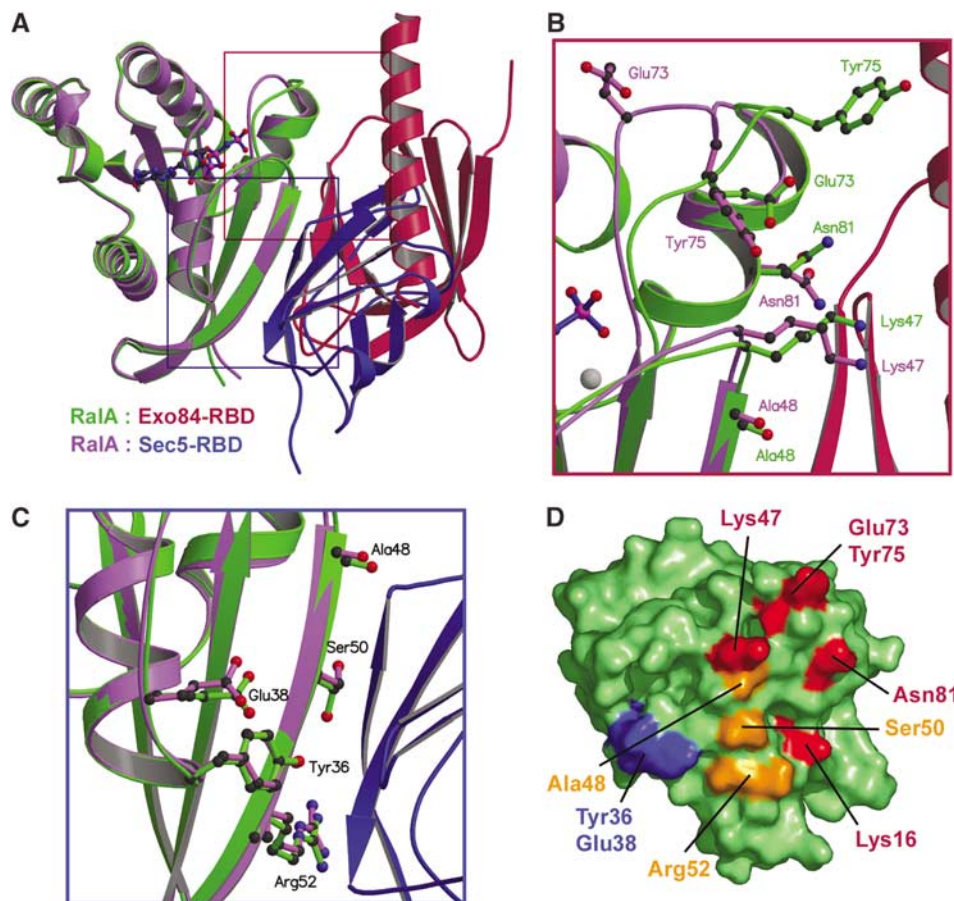
Figure 4 Exo84 and Sec5 have overlapping binding sites on the active RalA. (**A**) Superposition of the Exo84-RBD:RalA and the Sec5-RBD:RalA complexes. RalA is green in the Exo84-RBD:RalA complex and purple when in complex with Sec5-RBD. Exo84-RBD and Sec5-RBD are colored in red and blue, respectively. The two RalA molecules are superimposed using all equivalent Cα atoms except for residues in the two switch regions. Note that Exo84 and Sec5 cannot bind to RalA simultaneously. Close-up views of the areas that are indicated by red and blue boxes are shown in panels B and C, respectively. (**B**) Close-up view of the complex interface around RalA switch II where significantly different RalA conformations were observed between the two complexes. Shown are the five RalA residues in this region that directly contact Exo84-RBD. The molecules are colored as in panel A. (**C**) Close-up view of the Sec5-RBD:RalA interface. Shown are the five RalA residues that form hydrogen bonds with Sec5-RBD. The color scheme is the same as in panels A and B. (**D**) Molecular surface of RalA when it is in complex with Exo84-RBD. The RalA residues that exclusively contact Exo84-RBD are colored red, the residues that only bind Sec5-RBD are colored blue and the residues that are involved in interactions with both effectors are colored in orange.

Met238, Met241 and Ile252), which might compensate for the loss of two Arg52-mediated intermolecular hydrogen bonds. Indeed, when these two hydrogen bonds are abolished in the R52A^{RalA} mutant without providing additional hydrophobic interactions, the binding affinity between RalA and Exo84 decreases significantly. These results suggest distinct roles of Arg52^{RalA} for recognition of Exo84 or Sec5. When we mutated RalA residues that only participate in either pair of RalA–effector interactions, such as E38A^{RalA}, E38R^{RalA} or N81R^{RalA}, only the corresponding pair of effector–RalA interaction was affected. Taken together, our mutagenesis data are reminiscent of a phenomenon of so-called partial loss-of-function mutations in Ras, which renders Ras unable to activate some distinct effectors but not others.

Nucleotide- and effector-dependent conformational changes of RalA

Consistent with previous reports, we found that Exo84 only interacts with the active RalA (Table I). It is known that the switch regions of some small GTPases are mobile in the

inactive, GDP-bound form. However, all three available crystal forms of RalA-GDP structures show similar conformations in the switch regions, except for residues Gly71–Tyr75 (Bauer *et al*, 1999; Nicely *et al*, 2004). Specifically, the α-helix in switch II consisting of residues 76–84 is well defined and nearly identical in all three structures, even for the crystal form that exhibits no crystal packing contacts in this region (not shown). To determine the structural basis of GTP-dependent Exo84 binding, we thus superimposed the structure of the uncomplexed GDP-bound RalA (Bauer *et al*, 1999) on that of the GMPPNP-bound RalA in the context of the Exo84-RBD:RalA complex. The superposition reveals that the conformation of switch II in the GDP-bound state would impose severe steric hindrance for Exo84 binding (Figure 6). For example, RalA residues Tyr75, Ile78, Asn81 and Tyr82 would clash with the β4/β5 and the β6/β7 loops of Exo84-RBD. In addition, Asp49^{RalA} in switch I would collide with Asn231^{Exo84} and Lys233^{Exo84}.

The nucleotide-binding mode in the Exo84-RBD:RalA complex is essentially the same as that observed in the
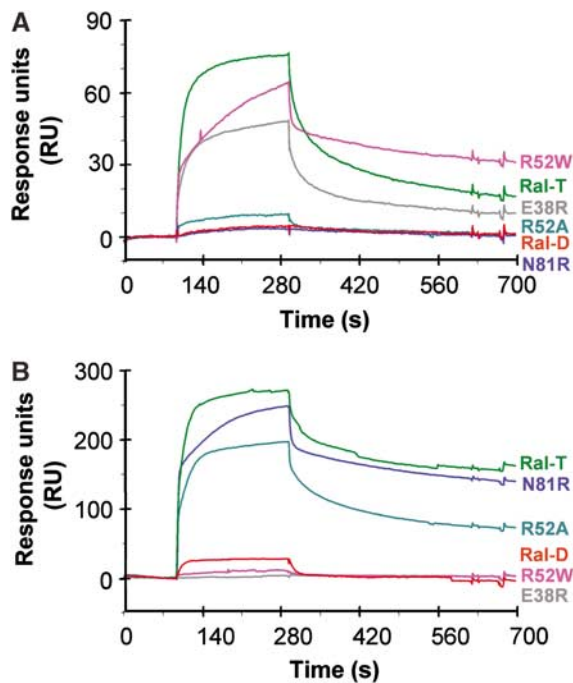
Figure 5 SPR measurements of RalA binding to Exo84-RBD and Sec5-RBD. Representative sensograms showing association and dissociation profiles of 500 nM GMPPNP- or GDP-bound RalA and its variants with wild-type Exo84-RBD (**A**) and Sec5-RBD (**B**). Ral-T indicates the GMPPNP-bound state and Ral-D the GDP-bound state. All other RalA mutants used were in the GMPPNP-bound state.

Sec5-RBD:RalA complex (Fukai *et al*, 2003), except for an additional hydrogen bond contributed by Tyr43[RalA]. We did not find evidence for a second Mg^{2+} associated with the γ-phosphate of GMPPNP as observed by Nicely *et al* (2004), suggesting that a second Mg^{2+} is not required for Exo84 binding. Comparison of the Exo84 and Sec5 complexes of the GMPPNP-bound RalA reveals a similar conformation of switch I (Cα atom r.m.s.d. of 0.62 Å), including residues that are involved in effector binding (Figure 4C). The only significant differences for RalA between the two complexes are observed for switch II residues 71–75 (Cα atom r.m.s.d. of 1.95 Å) (Figure 4B). Switch II does not directly participate in Sec5 binding and residues 72–75 are partially disordered in the Sec5-RBD:RalA complex (Fukai *et al*, 2003). As mentioned above, residues 71–75 show conformational variability in the GDP-bound RalA. Upon interaction with Exo84, a unique conformation is induced for residues 71–75 where Glu73 and Tyr75 directly interact with Exo84. The concomitant loss of entropy may be partially responsible for the relatively lower RalA binding affinity for Exo84 compared to that of Sec5. In summary, we find different types of conformational changes in RalA during activation and effector binding: the conformational changes in switch I and in α-helix 76–84 of switch II that set the stage for effector binding are mostly induced by activation, while the conformational changes of residues 71–75 are induced upon Exo84, but not Sec5, effector binding.

Binding specificity between Exo84 and RalA

Ral proteins are closely related to other members in the Ras superfamily according to their primary sequence homology. A primary sequence analysis showed that there are 14
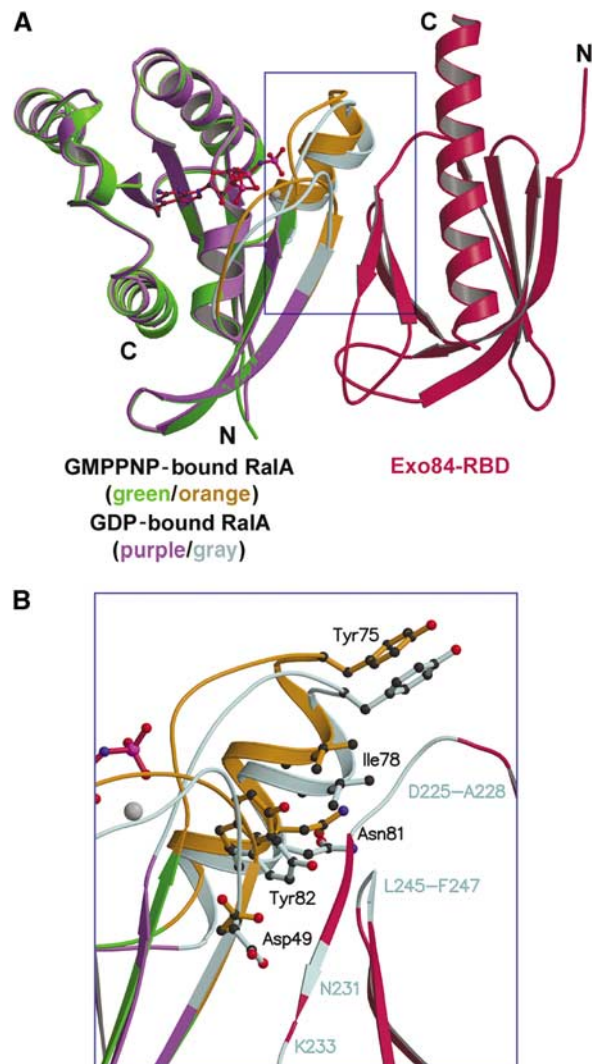
Figure 6 Exo84 selectively binds to the active RalA. (**A**) The GDP-bound RalA (purple) was superimposed on the GMPPNP-bound RalA (green) in the context of the Exo84-RBD:RalA complex. The two switch regions of the GMPPNP-bound and the GDP-bound RalA are colored in orange and gray, respectively. A close-up view of the boxed region is shown in panel B. (**B**) Close-up view of the area where some RalA residues in the GDP-bound conformation (gray), shown in a ball-and-stick representation, would clash with Exo84-RBD. Also shown is the corresponding conformation of RalA in the GMPPNP-bound state (orange). The Exo84 residues, which will potentially collide with the GDP-bound RalA, are colored in gray and labeled accordingly.

residues completely conserved in the Ral subfamily but differ in the other Ras subfamilies, which were termed Ral-tree-determinants (Bauer *et al*, 1999). Interestingly, four of these 14 residues (Lys47, Ala48, Ile78 and Asn81) are involved in Exo84 binding (Figure 3). We therefore focused on these four Ral-tree-determinants. Residues Ala48[RalA] and Ile78[RalA] are linked to the complex interface by Tyr82[RalA], which is sandwiched between these two residues. Tyr82[RalA] stabilizes the Exo84-RBD:RalA complex via a water-mediated hydrogen bond with Val229[Exo84], and hydrophobic interactions with Ala228, Val230 and Leu245 on Exo84. In comparison, Ras has Glu37 and Met67 in positions equivalent to Ala48[RalA] and Ile78[RalA]. Structural modeling revealed that the Ras-like conformation would force the side chain of Tyr82[RalA] to turn

away from the potential binding surface for Exo84, and therefore abolish the Tyr82-mediated Exo84–RalA interactions (not shown). Residue Asn81 is a unique feature of Ral, which helps to ensure the surface complementary between Ral and Exo84, as well as contributes two pairs of hydrogen bonds. Even a residue with a slightly larger side chain, such as its equivalent glutamine in Ras, would potentially collide with the neighboring Leu245[Exo84] and Met246[Exo84]. Indeed, when we introduced a larger residue at this position, such as N81R[RalA], the binding affinity decreased ∼21-fold. In contrast, Asn81-mediated hydrogen bonds only moderately strengthen the stability of the complex, since the N81A[RalA] mutant only decreases the binding affinity with Exo84 ∼1.5-fold. The positively charged Lys47 in Ral has been previously shown to represent a major difference between Ral and Ras regarding effector recognition, while Ras has a glutamate that is equivalent to Ala48[Exo84] (Bauer *et al*, 1999). Replacing Lys47[RalA] with a glutamate decreased the binding affinity with Exo84 ∼37-fold, since the K47E[RalA] mutant imposed an unfavorable charge interaction with the nearby Glu269[Exo84] and thus prevented RalA–Exo84 binding. In summary, we have identified four RalA residues (Lys47, Ala48, Ile78 and Asn81) that serve as specificity determinants for the Exo84–RalA interactions.

In order to identify key residues of Exo84 that are responsible for specific binding to RalA, we first carried out PSI-BLAST searches (Altschul *et al*, 1997) using full-length rat Exo84 as the bait. We found that Exo84 is highly conserved across different species (Figure 1). Most notably, we found a highly conserved motif, ^{228}AxxNx(K/R)D^{234}, of Exo84 where x refers to a small hydrophobic residue (typically Val or Ile) (Figure 1). This conserved motif comprises β5 and the two downstream residues of the Exo84-RBD (Figure 3C). The structure of the Exo84-RBD:RalA complex suggests that this motif is critical for the intermolecular interactions, as four residues in this region (Ala228, Val230, Asn231 and Lys233) are involved in RalA binding. This was confirmed by site-specific mutagenesis in this region (Exo84-A228W or K233W) and of corresponding interacting residues of RalA (RalA-A48W or S50W), which all dramatically decreased the Exo84–RalA binding affinity (Table I). In contrast to this highly conserved Exo84 motif, other Exo84 residues that are involved in Exo84–RalA binding are only moderately conserved (Figures 1 and 3D). When we mutated Ser276[Exo84] (S276W) or Lys272[Exo84] (K272A), only a marginal effect was observed regarding RalA binding (Table I). These results suggest that not all individual hydrogen bonds or salt bridges contribute significantly to the stability of the Exo84-RBD:RalA complex by itself. However, even weak interactions can add up to make a significant contribution to the binding affinity. For example, the Exo84-K272A and RalA-K47I mutants do not form a complex, even though they separately bind to the respective wild-type RalA or Exo84 with a wild-type-like binding affinity (Table I). In conclusion, we propose that the Exo84 residues in the highly conserved AxxNx(K/R)D motif are the major determinants for the specificity of the Exo84-RBD:RalA interactions.

Exo84 and Sec5 competitively bind to RalA in vitro

Since RalA interacts with two subunits in the same multimeric protein complex, these two pairs of interactions must be correlated. But, what is the relationship between them? As

shown in Figure 4, the binding sites for Exo84 and Sec5 on RalA are partially overlapping. Thus, Exo84 and Sec5 cannot bind to RalA simultaneously unless they would assume different binding modes. To confirm this structural prediction, competition experiments were carried out in solution (Figure 7). When the purified Exo84-RBD:RalA complex was incubated with excessive Sec5-RBD, a mixture of the Exo84-RBD:RalA and Sec5-RBD:RalA complexes was detected using size-exclusion chromatography (SEC). Meanwhile, a pool of free Exo84-RBD was observed that represented the Exo84-RBD expelled from the Exo84-RBD:RalA complex by Sec5-RBD. A similar result was observed when the preformed Sec5-RBD:RalA complex was mixed with excessive Exo84-RBD.

Conclusions

The unique cellular localizations of Exo84 and Ral provide a clue into the functional role of the Exo84–Ral interaction. In contrast to the other Sec6/8 subunits, Exo84 probably has a pool outside the fully assembled Sec6/8 complex (Guo *et al*, 1999; Moskalenko *et al*, 2003). We also observed that Exo84 is part of a larger soluble pool in comparison to other Sec6/8 subunits based on a detergent extraction of Sec6/8 subunits
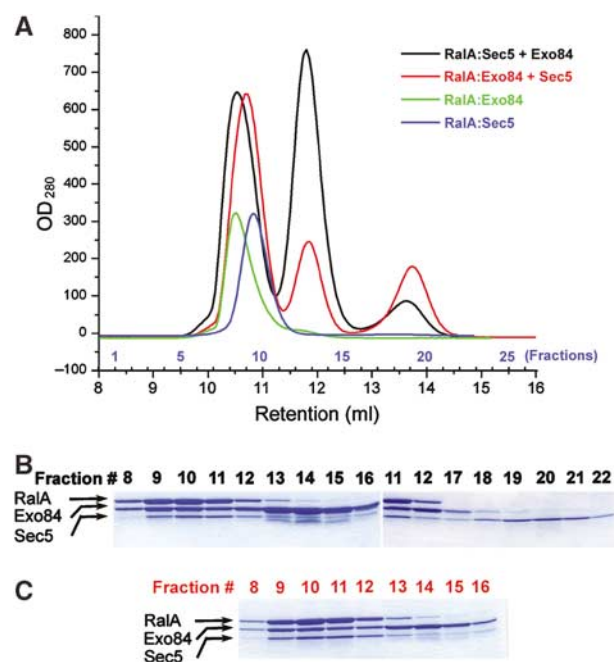
Figure 7 Exo84-RBD and Sec5-RBD competitively bind to the active RalA. The purified Exo84-RBD$^{146–289}$:RalA complex and the Sec5-RBD:RalA complex were mixed with excessive Sec5-RBD (red line) or Exo84-RBD (black line), respectively, and after incubation for several hours at 4°C, the mixture was resolved by a Superdex-75 (10/30) SEC column (Amersham) in a buffer containing 20 mM Tris, pH 7.5, 50 mM NaCl, 2 mM MgCl$_2$ and 1 mM DTT. The corresponding chromatograms are shown in (**A**) along with chromatograms of the purified Exo84-RBD$^{146–289}$:RalA (green) and Sec5-RBD:RalA (blue complexes). The OD$_{280}$ absorption curves were rescaled for better comparison. The peak fractions (0.3 ml each) were analyzed by SDS–PAGE for the competition experiment between the Sec5:RalA complex and Exo84 (**B**), and that between the Exo84:RalA complex and Sec5 (**C**). Similar results were observed for two Exo84-RBD constructs (residues 146–289 and 167–286).

with rat brain extract (data not shown). Furthermore, seven Sec6/8 subunits *excluding* Exo84 can associate with each other to form a subcomplex *in vitro* (Wang *et al*, 2004b). However, inhibition of endogenous Exo84 expression reduced the formation of the Sec6/8 complex (Moskalenko *et al*, 2003). It suggests that Sec6/8 complexes are assembled from subcomplexes, probably mediated in part by Exo84. On the other hand, due to its carboxy-terminal geranylation, Ral associates with secretory compartments and the plasma membrane (Mark *et al*, 1996). Functionally, Ral is an important regulator of vesicle trafficking and crucial for the assembly of the Sec6/8 complex (Moskalenko *et al*, 2002). Here, we have provided structural and biochemical evidence that Exo84 and Sec5 competitively bind to active Ral. Taken together, this suggests that there are at least two different Sec6/8 subcomplexes that contain Exo84 and Sec5, respectively, and the Sec6/8 assembly is regulated by Ral interactions with Exo84 and Sec5.

A Sec5-containing subcomplex has been proposed to be located on the target plasma membrane, serving as a landmark site for exocytosis (Moskalenko *et al*, 2003). In response to a specific cellular signal, Ral is thought to be activated and to recruit the Exo84-containing subcomplex to the vesicle membrane. The Exo84-containing subcomplex and its associated vesicle are then delivered to a specific region on the plasma membrane, which is tagged by the Sec5-containing subcomplex. This vesicle trafficking process is likely mediated by Ral, and may be in coordination with the cytoskeleton and/or other regulators. The subsequent assembly of the Sec6/8 complex will therefore bridge secretory vesicles to their target membrane. Since Exo84 and Sec5 can directly associate with each other via regions that are distinct from their RBDs, the Exo84–Sec5 interaction is probably independent of the Exo84–Ral and Sec5–Ral interactions (Moskalenko *et al*, 2003). It has been shown that at least one Ral-GTP molecule binds the Sec6/8 complex (Sugihara *et al*, 2002; Wang *et al*, 2004a), although the available data cannot distinguish if one or two Ral molecules bind to the fully assembled Sec6/8 complex. The structural and biochemical insights that we have obtained about RalA–Sec6/8 interactions have shed new light on the ability of Ral to interact with two different effectors that can also be part of the same multiprotein complex. Taken together, our results further strengthen the proposed role of Ral-regulated assembly of the Sec6/8 complex.

Materials and methods

Cloning, protein expression and purification
Various constructs of rat Exo84-RBD and human RalA (residues 9–183) were cloned into the pGEX-2T vector (Amersham) and expressed as GST fusion proteins in *Escherichia coli* BL-21 cells. The Q72L mutation on RalA was introduced by site-directed mutagenesis (QuikChange, Stratagene). To probe the domain structure and boundaries of the RBD of Exo84, we have screened 17 different truncations of Exo84 covering the N-terminal 389 residues. The designs of various Exo84-RBD constructs were guided by information gathered from limited proteolysis, N-terminal amino-acid sequencing and liquid chromatography/mass spectrometry (LC–MS). Soluble proteins were further tested for binding with active RalA using a GST pull-down assay. For expression of each protein, bacteria were grown at 37°C and induced with 100 μM of isopropyl-β-D-thiogalactopyranoside (IPTG) when OD_{600} absorption reached 0.6–0.8. The temperature was then reduced to 20°C and the induction was continued for ~16 h. Cells were harvested and resuspended in phosphate-buffered saline (PBS) buffer with 2 mM dithiothreitol (DTT), 5 mM EDTA, 0.5 mM PMSF and protease inhibitor cocktail (Roche), and lysed by a microfluidizer (Micro-fluidics Corporation). The clarified cell lysate was loaded to a glutathione-Sepharose 4B column (Amersham) at 4°C, and then washed extensively with a buffer containing 50 mM Tris, pH 8.0, 150 mM NaCl and 2 mM DTT. GST fusion Exo84-RBD and RalA were cleaved with thrombin (Hematologic Technology) on the column. Exo84-RBD was used for complex formation with RalA without further purification. RalA was further purified using a 5 ml HiTrap-Q column (Amersham) which was pre-equilibrated with 50 mM Tris, pH 7.5, 1 mM $MgCl_2$ and 1 mM DTT, and subsequently eluted with an NaCl gradient (0–0.4 M). To convert RalA to the GTP-bound form with GMPPNP, a nonhydrolyzable GTP analog (Calbiochem), purified RalA was incubated with calf intestinal alkaline phosphatase (10 U/mg RalA) (CIP, New England Biolabs), 0.5 mM GMPPNP, together with 5 mM EDTA and 50 mM ammonium sulfate. Nucleotide exchange lasted for 16 h at 4°C and was stopped by adding 10 mM $MgCl_2$. The complex was formed by mixing GMPPNP-loaded RalA with purified Exo84-RBD. After incubating at 4°C overnight, the mixture of Exo84-RBD and RalA was loaded on a 5 ml HiTrap-Q column pre-equilibrated with a buffer containing 50 mM Tris, pH 7.5, 1 mM $MgCl_2$ and 1 mM DTT. The Exo84-RBD:RalA complex was eluted with a 0–0.4 M NaCl gradient, and was further purified by a HiLoad-16/60 Superdex-75 (Amersham) size-exclusion column in a buffer composed of 20 mM Tris, pH 7.5, 50 mM NaCl, 2 mM $MgCl_2$ and 1 mM DTT.

Selenomethionyl Exo84-RBD (residues 167–286) (Se-Met Exo84-RBD) was expressed by growing cells in M9 minimum media supplemented with amino acids Lys, Phe, Thr, Ile, Leu, Val and Se-Met (Doublie, 1997). Se-Met Exo84-RBD was purified using the same protocol as for the native protein, except that 10 mM DTT was included throughout protein purification. Complex was formed between Se-Met Exo84-RBD and native RalA.

Crystallization and diffraction data collection
The purified Exo84-RBD:RalA complex was concentrated to ~20 mg/ml for crystallization. Initial crystallization screens were carried out using crystallization screen kits from Hampton Research and Emerald Biostructures. The best crystals were grown at 20°C by vapor diffusion, and each drop contained a 1:1 (v/v) ratio of protein and reservoir solution. The reservoir solution was composed of 18–22% PEG3350, 0.1–0.2 M ammonium sulfate and 0.1 M Bis–Tris buffer, pH 6.5. Clusters of thin plates grew in 1–2 weeks and diffraction quality crystals were grown using microseeding. The complex of Se-Met Exo84-RBD and native RalA was crystallized in a similar condition in the presence of 10 mM DTT. However, it only crystallized after cross-seeding using crystals of native complex.

The crystals were cryoprotected in the same mother liquor supplemented with 13% glycerol, and then flash-frozen in liquid nitrogen. The diffraction data sets were collected at 100 K at beam lines 9-2 and 11-1, Stanford Linear Accelerator Center (SSRL), using an ADSC Q315 CCD detector. A three wavelength multiwavelength anomalous dispersion (MAD) data sets were collected using inverse-beam geometry in 10° wedges. All data were processed using HKL2000 (Table II) (Otwinowski and Minor, 1997). The crystals belonged to space group P2₁. The Se-Met crystals were isomorphous with the native crystals.

Structure determination
The positions of 11 of the 12 possible selenium sites were found using the program SOLVE (Terwilliger and Berendzen, 1999). MAD phasing and subsequent density modification were carried out in the Crystallography & NMR System (CNS) (Brunger *et al*, 1998). The computed experimental electron density map was of excellent quality and allowed unambiguous tracing for most of the protein backbone and side chains in the Exo84-RBD[167–286]:RalA complex. An initial model was built using the program O into the 2.5 Å resolution electron density map calculated from MAD phases (Jones *et al*, 1991). The electron density improved by iterative manual rebuilding and refinement with CNS, against the 2.5 Å resolution data. Progress was monitored with the free *R*-value using a 10% randomly selected test set (Brunger, 1992). The loop between Leu209 and Met215 was still missing when the conventional *R*-value was 0.260 and the *R*-free value was 0.306. At this point, the structure of Exo84-RBD[167–279]:RalA, with a diffraction data to 2.0 Å, was determined by molecular replacement with AmoRe (Navaza,

1994), using the Exo84-RBD$^{167-286}$:RalA structure as a search model. Refinements were begun with rigid body minimization followed by a slow-cooling simulated annealing protocol at 5000 K to reduce model bias. The structure of the missing loop between 209 and 215 could now be reliably assigned using this high-resolution data, although the electron density map was relatively weak in this region. Iterative rounds of positional and individual *B*-factor refinement were performed in conjunction with manual model building until R_{free} converged. The ligands were not included until R_{free} was under 0.30. The missing loop in the Exo84-RBD$^{167-286}$: RalA complex was built using the Exo84-RBD$^{167-279}$:RalA structure as a reference. The final models are complete except for weak or missing electron density for the four N-terminal residues and the three C-terminal residues of Exo84-RBD$^{167-286}$, the four N-terminal residues of Exo84-RBD$^{167-279}$ and the two N-terminal residues of RalA. The occupancy of residue Arg213^{Exo84} in the Exo84-RBD$^{167-286}$:RalA complex was set to zero because of the weak electron density. For structure comparison, least-squares superpositions were calculated using LSQMAN (Kleywegt, 1999). Figures were prepared using programs MOLSCRIPT (Kraulis, 1991), PyMol (http://www.pymol.org), Povscript (http://www.stanford.edu/~fenn/povscript/) and Raster3D (Merritt and Murphy, 1994).

The atomic coordinates and diffraction data for the Exo84-RBD$^{167-279}$:RalA and Exo84-RBD$^{167-286}$:RalA structures have been deposited at the Protein Data Bank under accession codes 1ZC3 and 1ZC4, respectively.

Molecular weight determination by multiangle laser light scattering

An HR 10/30 Superdex-75 (Amersham) SEC column was coupled with in-line DAWN EOS multiangle light scattering, refractive index (Wyatt Technology Corporation) and UV (Jasco Corporation) detectors (SEC-MALLS). The system was equilibrated in 20 mM Tris, pH 7.5, 50 mM NaCl and 2 mM MgCl$_2$. The protein concentrations were about 3 mg/ml and the flow rate was maintained at 0.35 ml/min. The light scattering detector responses were calibrated by measuring the signals from monomeric bovine serum albumin. The light scattering unit was maintained at 25°C and the refractometer was maintained at 35°C. The column and all external connections were at ambient temperature (20–22°C). A value of 0.185 ml/g was assumed for the dn/dc value of the proteins. The native molecular weight of the eluted species was calculated using the ASTRA 4.90.08 software provided by Wyatt Technology Corporation.

Mutagenesis and binding analysis

Single site-specific mutations were introduced into the full-length human RalA and rat Exo84-RBD (167–286) by PCR. Thrombin-cleaved GMPPNP- or GDP-bound RalA and its variants were purified as described previously (Fukai *et al*, 2003). Exo84-RBD and its variants were purified as described above, and the identity of the Exo84-RBD mutants was confirmed by mass spectrometry. Binding affinities were determined by SPR measurements on a BIAcore 3000 instrument (Biacore Inc.). Wild type or mutant forms of Exo84-RBD or Sec5-RBD were coupled to activated CM5 surfaces using standard amine coupling conditions as described by the manufacturer. Exo84-RBD variants or Sec5-RBD were captured on flow cells 2–4 at a level of 600–800 response units (RU) and flow cell 1 was used as a reference cell by not coupling any protein to it. Sensograms were recorded at 25°C for binding of RalA and its variants to these surfaces by injection of series of solutions ranging from 50 to 10 000 nM in the presence of 0.2 mM of GMPPNP or GDP. Kinetic injections were carried out by allowing 200 s for association and 600 s for dissociation at a flow rate of 30 μl/min (PBS running buffer: PBS, pH 7.2, containing 2.5 mM MgCl$_2$, 0.05% Tween 20 and 0.02% sodium azide). Exo84-RBD/Sec5-RBD biosensor surfaces were regenerated with 100 μl of PBS containing 50 mM EDTA. The signal from the reference cell for the same injection was subtracted from the observed sensogram. A 600 RU of coupled Exo84-RBD/ Sec5-RBD would routinely result in a response of 80 and 250 RU with 500 nM GMPPNP-bound RalA, respectively. Dissociation constants (K_d) were derived by fitting the data into 1:1 Langmuir binding model using the BIAevaluation 3.2 software (Biacore Inc.). This model describes a simple reversible interaction of two molecules in a 1:1 complex. All binding experiments were repeated three to four times and biosensor chips coupled at different times yielded comparable binding affinities. Experiments in opposite orientation using RalA coupled to the chip were not successful as nucleotide-bound RalA could not be maintained during the regeneration, thereby creating inactive RalA species on chip. The K_d values for Sec5-RBD:RalA interaction reported here (as measured by BIAcore analysis) were 10 times lower (affinity is stronger) compared to previously reported values that were measured by isothermal titration calorimetric analysis (Fukai *et al*, 2003). This difference could be attributed to different methods used for the analysis.

Supplementary data

Supplementary data are available at *The EMBO Journal* Online.

References

Altschul SF, Madden TL, Schaffer AA, Zhang J, Zhang Z, Miller W, Lipman DJ (1997) Gapped BLAST and PSI-BLAST: a new generation of protein database search programs. *Nucleic Acids Res* **25:** 3389–3402

Bauer B, Mirey G, Vetter IR, Garcia-Ranea JA, Valencia A, Wittinghofer A, Camonis JH, Cool RH (1999) Effector recognition by the small GTP-binding proteins Ras and Ral. *J Biol Chem* **274:** 17763–17770

Brunger AT (1992) Free *R*-value: a novel statistical quantity for assessing the accuracy of crystal structures. *Nature* **355:** 472–475

Brunger AT, Adams PD, Clore GM, DeLano WL, Gros P, Grosse-Kunstleve RW, Jiang JS, Kuszewski J, Nilges M, Pannu NS, Read RJ, Rice LM, Simonson T, Warren GL (1998) Crystallography & NMR system: a new software suite for macromolecular structure determination. *Acta Crystallogr D* **54** (Part 5)**:** 905–921

Doublie S (1997) Preparation of selenomethionyl proteins for phase determination. *Methods Enzymol* **276:** 523–530

Feig LA (2003) Ral-GTPases: approaching their 15 min of fame. *Trends Cell Biol* **13:** 419–425

Ferguson KM, Kavran JM, Sankaran VG, Fournier E, Isakoff SJ, Skolnik EY, Lemmon MA (2000) Structural basis for discrimination of 3-phosphoinositides by pleckstrin homology domains. *Mol Cell* **6:** 373–384

Frech M, Darden TA, Pedersen LG, Foley CK, Charifson PS, Anderson MW, Wittinghofer A (1994) Role of glutamine-61 in the hydrolysis of GTP by p21H-ras: an experimental and theoretical study. *Biochemistry* **33:** 3237–3244

Fukai S, Matern HT, Jagath JR, Scheller RH, Brunger AT (2003) Structural basis of the interaction between RalA and Sec5, a subunit of the sec6/8 complex. *EMBO J* **22:** 3267–3278

Glaser F, Pupko T, Paz I, Bell RE, Bechor-Shental D, Martz E, Ben-Tal N (2003) ConSurf: identification of functional regions in proteins by surface-mapping of phylogenetic information. *Bioinformatics* **19:** 163–164

Grindstaff KK, Yeaman C, Anandasabapathy N, Hsu SC, Rodriguez-Boulan E, Scheller RH, Nelson WJ (1998) Sec6/8 complex is recruited to cell–cell contacts and specifies transport vesicle delivery to the basal–lateral membrane in epithelial cells. *Cell* **93:** 731–740

Guo W, Grant A, Novick P (1999) Exo84p is an exocyst protein essential for secretion. *J Biol Chem* **274:** 23558–23564

Inoue M, Chang L, Hwang J, Chiang SH, Saltiel AR (2003) The exocyst complex is required for targeting of Glut4 to the plasma membrane by insulin. *Nature* **422:** 629–633

Jahn R, Südhof TC (1999) Membrane fusion and exocytosis. *Annu Rev Biochem* **68:** 863–911

Jones TA, Zou JY, Cowan SW, Kjeldgaard M (1991) Improved methods for building protein models in electron density maps and the location of errors in these models. *Acta Crystallogr A* **47** (Part 2)**:** 110–119

Kee Y, Yoo JS, Hazuka CD, Peterson KE, Hsu SC, Scheller RH (1997) Subunit structure of the mammalian exocyst complex. *Proc Natl Acad Sci USA* **94:** 14438–14443

Kleywegt GJ (1999) Experimental assessment of differences between related protein crystal structures. *Acta Crystallogr D* **55:** 1878–1884

Kraulis PJ (1991) MOLSCRIPT: a program to produce both detailed and schematic plots of protein structures. *J Appl Crystallogr* **24:** 946–950

Lemmon MA, Ferguson KM (2000) Signal-dependent membrane targeting by pleckstrin homology (PH) domains. *Biochem J* **350** (Part 1)**:** 1–18

Mark BL, Jilkina O, Bhullar RP (1996) Association of Ral GTP-binding protein with human platelet dense granules. *Biochem Biophys Res Commun* **225:** 40–46

Matern HT, Yeaman C, Nelson WJ, Scheller RH (2001) The Sec6/8 complex in mammalian cells: characterization of mammalian Sec3, subunit interactions, and expression of subunits in polarized cells. *Proc Natl Acad Sci USA* **98:** 9648–9653

Merritt EA, Murphy MEP (1994) Raster3D Version 2.0. A program for photorealistic molecular graphics. *Acta Crystallogr D* **50:** 869–873

Moskalenko S, Henry DO, Rosse C, Mirey G, Camonis JH, White MA (2002) The exocyst is a Ral effector complex. *Nat Cell Biol* **4:** 66–72

Moskalenko S, Tong C, Rosse C, Mirey G, Formstecher E, Daviet L, Camonis J, White MA (2003) Ral GTPases regulate exocyst assembly through dual subunit interactions. *J Biol Chem* **278:** 51743–51748

Navaza J (1994) AMoRe: an automated package for molecular replacement. *Acta Crystallogr A* **50:** 157–163

Nicely NI, Kosak J, de Serrano V, Mattos C (2004) Crystal structures of Ral-GppNHp and Ral-GDP reveal two binding sites that are also present in Ras and Rap. *Structure (Camb)* **12:** 2025–2036

Novick P, Guo W (2002) Ras family therapy: Rab, Rho and Ral talk to the exocyst. *Trends Cell Biol* **12:** 247–249

Otwinowski Z, Minor W (1997) Processing of X-ray diffraction data collected in oscillation mode. *Methods Enzymol* **276:** 307–326

Pacold ME, Suire S, Perisic O, Lara-Gonzalez S, Davis CT, Walker EH, Hawkins PT, Stephens L, Eccleston JF, Williams RL (2000) Crystal structure and functional analysis of Ras binding to its effector phosphoinositide 3-kinase gamma. *Cell* **103:** 931–943

Prigent M, Dubois T, Raposo G, Derrien V, Tenza D, Rosse C, Camonis J, Chavrier P (2003) ARF6 controls post-endocytic recycling through its downstream exocyst complex effector. *J Cell Biol* **163:** 1111–1121

Sugihara K, Asano S, Tanaka K, Iwamatsu A, Okawa K, Ohta Y (2002) The exocyst complex binds the small GTPase RalA to mediate filopodia formation. *Nat Cell Biol* **4:** 73–78

TerBush DR, Maurice T, Roth D, Novick P (1996) The Exocyst is a multiprotein complex required for exocytosis in *Saccharomyces cerevisiae*. *EMBO J* **15:** 6483–6494

Terwilliger TC, Berendzen J (1999) Automated MAD and MIR structure solution. *Acta Crystallogr D* **55** (Part 4)**:** 849–861

Thompson JD, Higgins DG, Gibson TJ (1994) CLUSTAL W: improving the sensitivity of progressive multiple sequence alignment through sequence weighting, position-specific gap penalties and weight matrix choice. *Nucleic Acids Res* **22:** 4673–4680

Vega IE, Hsu SC (2001) The exocyst complex associates with microtubules to mediate vesicle targeting and neurite outgrowth. *J Neurosci* **21:** 3839–3848

Vetter IR, Wittinghofer A (2001) The guanine nucleotide-binding switch in three dimensions. *Science* **294:** 1299–1304

Wang L, Li G, Sugita S (2004a) RalA–exocyst interaction mediates GTP-dependent exocytosis. *J Biol Chem* **279:** 19875–19881

Wang S, Liu Y, Adamson CL, Valdez G, Guo W, Hsu SC (2004b) The mammalian exocyst, a complex required for exocytosis, inhibits tubulin polymerization. *J Biol Chem* **279:** 35958–35966

Whyte JR, Munro S (2002) Vesicle tethering complexes in membrane traffic. *J Cell Sci* **115:** 2627–2637

Zhang XM, Ellis S, Sriratana A, Mitchell CA, Rowe T (2004) Sec15 is an effector for the Rab11 GTPase in mammalian cells. *J Biol Chem* **279:** 43027–43034